

MULTIFREQUENCY RADAR SIGNALS

Nadav Levanon, Dept. of Elect. Eng. – Systems, Tel Aviv University, Tel Aviv, Israel

Abstract

A multifrequency radar signal is considered. It employs M subcarriers *simultaneously*. The subcarriers are phase modulated by M different sequences that constitute a *complementary* set. Such a set can be constructed, for example, from the M cyclic shifts of a perfect phase-coded sequence of length M (e.g., P4). The subcarriers are separated by the inverse of the duration of a phase element t_b , yielding Orthogonal Frequency Division Multiplexing (OFDM), well known in communications. The signal exhibits a thumbtack ambiguity function with delay resolution of t_b/M . The power spectrum is relatively flat, with width of M/t_b . The signal can be constructed by power combining M fixed-amplitude signals. The resulting signal, however, is of variable amplitude.

Introduction

Range (delay) resolution is inversely related to the radar signal bandwidth. The quest for higher bandwidth usually follows shorter bit duration in digital phase modulated signals, or wider frequency deviation in analog frequency modulated signals. In radio communications, which faces similar quest for bandwidth, one solution is the use of a modulation technique known as Orthogonal Frequency Division Multiplexing (OFDM). The basic idea of OFDM is to replace transmitting serially M short modulation symbols, each of duration t_c , by transmitting M long symbols, each of duration $t_b = Mt_c$, in parallel, on M different subcarriers. In OFDM the subcarriers are separated by $1/t_b$ which ensures that the subcarrier frequencies are orthogonal and phase continuity is maintained from one symbol to the next. OFDM is the suggested technique for Digital Audio Broadcasting [1].

Simultaneous use of several subcarriers in radar was recently reported by Jankiraman *et al.*[2]. The PANDORA[2] FMCW radar achieves bandwidth of 384 MHz, by using 8 Linear-FM (LFM) channels, each sweeping 48 MHz. Together with guard bands, the bandwidth totals 776 MHz. A multifrequency signal is characterized by varying amplitude. Amplifying such a signal requires linear power amplifiers (LPA), which are relatively inefficient. Much of Jankiraman's paper is devoted to issues of power combining and amplification.

A modern replacement of the analog LFM signal is a digital phase-coded signal, in particular the P3 and P4 signals [3], whose phase sequences are samples from the phase history of a LFM signal.

An analogy to the FMCW multifrequency approach would have suggested repeating the same phase-coded modulation sequence on all M subcarriers. We found that lower autocorrelation sidelobes are reached when the M sequences are different from each other and constitute a complementary set. We will call such a signal Multifrequency Complementary Phase Coded (MCPC) signal of size $M \times M$. This paper describes several versions of the MCPC signal and compares its performances to P4, Huffman [4,5] and Costas [6] signals.

MCPC Based on All Cyclic Shifts of P4

The phase sequence of a P4 signal is described by

$$\phi_m = \frac{\pi}{M}(m-1)^2 - \pi(m-1), \quad m = 1, 2, \dots, M \quad (1)$$

P4 and P3 signals exhibit ideal periodic autocorrelation, namely zero periodic autocorrelation sidelobes. Deducing from simultaneous transmission of LFM pulses would have led us to suggest repeating the same phase sequence on all M subcarriers. However phase coded signals yield an additional degree of freedom in the form of cyclic shift. Popovic [7] has shown that *all the different cyclic time shifted versions of any sequence having an ideal periodic autocorrelation function, form a complementary set*.

A complex valued sequence X_i , whose k^{th} element is $s_i(k)$, forms a complementary set if the sum $Z(p)$ of the a -periodic autocorrelation function R_i of all sequences from the set is equal to zero for all nonzero time shifts p , i.e.,

$$Z(p) = \sum_{i=0}^{M-1} \sum_{k=0}^{M-1-p} s_i(k)s_i^*(k+p) = \begin{cases} \sum_{i=0}^{M-1} R_i(0), & p=0 \\ 0, & p \neq 0 \end{cases} \quad (2)$$

where $*$ denotes complex conjugate, p is the (positive) time shift, and $R_i(0)$ is the energy of the sequence X_i .

When the set has only two sequences (a complementary pair), the two sequences (of equal length M) must have aperiodic autocorrelation functions whose sidelobes are equal in magnitude but opposite in sign. The sum of the two autocorrelation functions has a peak of $2M$ and a sidelobe level of zero.

In order to take advantage of this autocorrelation property in radar signals [8], the sequences must be separated, e.g., in time (two different pulses). With large time

separation, even small Doppler shift causes large phase shift, and the sequences quickly lose the property of cancelled autocorrelation sidelobes.

The use of multiple subcarriers provides another possibility of separation – frequency. We will investigate the properties of such a signal using a simple complementary set constituted of the 5 shifts of a P4 signal of length 5. The basic phase sequence is obtained by using $M=5$ in (1). It appears in the top row of Table 1. The remaining rows are all the remaining cyclic shifts.

Table 1. Set of 5 complementary phase coded sequences

Seq. 1	0°	-144°	-216°	-216°	-144°
2	-144°	-216°	-216°	-144°	0°
3	-216°	-216°	-144°	0°	-144°
4	-216°	-144°	0°	-144°	-216°
5	-144°	0°	-144°	-216°	-216°

Following the OFDM approach, the M ($=5$) sequences will be transmitted on M subcarriers, separated by $f_s = 1/t_b$, where t_b is the duration of each phase element (bit). The complex envelope of the transmitted signal is therefore

$$u(t) = \begin{cases} \sum_{n=1}^M \exp\{j[2\pi f_s(\frac{M+1}{2} - n) + \theta_n]\} \sum_{m=1}^M u_{n,m}[t - (m-1)t_b], & 0 \leq t \leq Mt_b \\ 0, & \text{elsewhere} \end{cases} \quad (3)$$

where

$$u_{n,m}(t) = \begin{cases} \exp(j\phi_{n,m}), & 0 \leq t \leq t_b \\ 0, & \text{elsewhere} \end{cases} \quad (4)$$

$\phi_{n,m}$ is the m^{th} phase element of the n^{th} sequence, and θ_n is an arbitrary phase shift added by the transmitter hardware to each carrier (known to the receiver). (3) and (4) describe the complex envelope of $M \times M$ MCPC signal.

Comparison Between $M \times M$ MCPC ($M=5$) and P4 ($N=25$)

Fig. 1 compares schematically a 25 chip P4 signal (left) and a 5×5 MCPC signal (right). The P4 signal is constructed from N phase modulation chips, each of duration t_c . The typical autocorrelation of a P4 signal exhibit a narrow main lobe at zero delay, a first null at t_c , and low sidelobes extending as far as the signal duration Nt_c . The power spectral density of P4 resembles a $\sin^2(\pi f t_c) / (\pi f t_c)^2$ function. The first null is at $f = 1/t_c$ and the spectrum peak sidelobe level is -26 dB.

The schematic description of the MCPC signal (r.h.s. of Fig. 1), shows M ($=5$) sequences modulating M subcarriers. The bit duration t_b in each sequence was chosen to be M times longer than t_c . This will yield an autocorrelation mainlobe width similar to a P4 signal with M^2 ($=25$) chip. We will also show that the MCPC signal exhibits a more efficient spectrum usage. As depicted in Fig. 1, the power spectrum is nearly rectangular with cutoff at $f \approx M/(2t_b)$.

The ambiguity function and its zero-Doppler cut (the magnitude of the autocorrelation) of $u(t)$ depends on the permutation of the 5 sequences along the 5 subcarriers ($2f_s, f_s, 0, -f_s, -2f_s$). A preferred (low sidelobe RMS) permutation results in the autocorrelation (magnitude) shown in Fig. 2. Note that the first null appears at $t_b/5$. This means that by using 5 subcarriers we have created an autocorrelation resembling that of a signal that, over the same duration, has 5 times as many bits. Indeed it is interesting to compare the autocorrelation in Fig. 2 with the autocorrelation of a P4 signal of length 25. Its magnitude is plotted in Fig. 3. The phase sequence of a P4 signal with 25 elements uses 13 distinct phase values. This compares with only 3 distinct values in Table 1. Two other interesting aspects to compare are the occupied spectrum and the Doppler sensitivity. The power spectral density (PSD) of the MCPC signal, obtained from the Fourier transform of the autocorrelation in Fig. 2, is presented in Fig. 4. The PSD of the P4 signal (25 elements) is given in Fig. 5. In general the MCPC signals exhibit a more narrow and flat spectrum (of the complex envelope) extending as far as

$$f_{\max} \approx \frac{M}{2t_b} \quad (5)$$

The bandwidth of the band-pass signal around its center frequency will therefore be

$$\text{BW} = 2f_{\max} \approx \frac{M}{t_b} \quad (6)$$

The sensitivity to Doppler shift is described by the ambiguity function. The 1st and 2nd quadrants are shown in Fig. 6 for the 5×5 MCPC signal, and in Fig. 7 for the 25 element P4 signal. The ambiguity function of the MCPC signals does not exhibit the ridge seen in the ambiguity function of the P4 signal (also typical of LFM). Zooming will reveal that there is no rapid increase of the sidelobe level with small Doppler shift.

The performances of the MCPC signal were calculated assuming no hardware inserted phase shifts, namely, in (3) we assumed $\theta_n = 0, n = 1, \dots, M$. Phase shifts other than zero will slightly modify the spectrum and the sidelobe patterns of the ambiguity function. The resulting effect will be similar to that of using a different sequence order.

Comparison Between $M \times M$ MCPC ($M=9$) And P4 ($N=25$)

From a spectral width point of view it is more reasonable to compare the 25 element P4 signal with a 9×9 MCPC signal. The sequence order of the MCPC signal is that order which yields the lowest RMS sidelobe level, found by an exhaustive search. (valid as long as $\theta_n = 0$, $n = 1, \dots, M$). The autocorrelation (in dB) of both signals is given in Fig. 8. It reveals a similar peak-sidelobe level of -20 dB, yet a much narrower mainlobe of the MCPC signal. The ratio of the first delay nulls is

$$\frac{\tau_{\text{null, MCPC}}}{\tau_{\text{null, P4}}} = \frac{N}{M^2} = \frac{25}{81} \approx 0.3 \quad (7)$$

Studying MCPC signals of other sizes reveals a clear sidelobe level drop as M increases. For $M \leq 13$, an empirical relationship of the sidelobe RMS value in dB is $20 \log(SL_{\text{RMS}}) \approx -(1.13M + 17.7)$. The best found permutations were used to obtain the relationship. However, for $M \geq 11$ the large number of permutations ($11! \approx 4 \cdot 10^7$) excludes an exhaustive search. The large number of permutations could be exploited when many similar radars must coexist in physical proximity, e.g., in automotive radar applications.

Train of Complementary MCPC Pulses

A train of M MCPC pulses can be complementary in time as well as in frequency. Each pulse exhibits a different order of sequences in order to achieve a set of complementary phase sequences in each frequency. The autocorrelation sidelobes are further reduced as demonstrated in Fig. 9 (for $M=5$). The order of sequences is outlined within the drawing.

MCPC Based on 2-valued Complementary Set

The P4 phase sequence used so far to construct the MCPC complementary set is a polyphase code. There are 2-valued phase sequences that also exhibit perfect periodic autocorrelation, and can serve to construct a complementary set. One such alternative is the sequences described by Golomb [9]. One example of such a sequence is based on Barker code of length 7 [$+++--$], in which the two phase values are not 0 and 180° but 0 and 138.59° ($= \arccos(-3/4)$). Codes of this type exist for lengths 3, 7, 11, 15, 19, 23, 31, 35, 43, 47, 59, ... For a 11×11 MCPC signal based on all the cyclic shifts of the corresponding two-valued perfect sequence, the autocorrelation (magnitude) and the ambiguity function are presented in Figs. 10 and 11 respectively. The RMS sidelobe value of the two-valued signal is usually 15% higher than for a polyphase signal of the same size.

It is also interesting to compare the autocorrelation of the two-valued signal with one in which the phase values were changed to 0 and 180° (not a complementary set any more, but easier to implement). Degradation in RMS value by about 25% (relative to the ideal two-valued code) is typical. In all MCPC signals based on complementary sets the autocorrelation is identically zero at multiples of t_b . This property is lost in a non complementary set, and is one reason for the higher sidelobe RMS value.

Implementing two-valued sequences is especially simple if the two are binary values ($-1, +1$). There are only few square or nearly-square binary complementary sets. Some examples are listed below [10].

+++	++++	++--	+----
-++	+--+	+---	-++--
+--	+---	-+++	+----
+--	+---	+++--	-----

Comparison with Huffman Coded Signals

A single phase-modulated carrier exhibits constant amplitude while a multicarrier signal exhibits varying amplitude. The real envelope of a 5×5 MCPC signal is shown in Fig. 12. Amplifying such a signal requires a linear amplifier. Linear power amplifiers (LPA) are not as efficient as non-linear amplifiers that can be used for amplifying constant amplitude signals. This is a major drawback of the MCPC signal. However, there is continuing progress in microwave power modules that makes varying amplitude radar signals more practical. This is especially true for low power radars using solid state devices.

The variable amplitude of the MCPC signal invites comparison with Huffman-coded signals [4,5]. Huffman signals are constructed from N elements of width t_c , each one modulated in amplitude as well as in phase. The result is nearly ideal autocorrelation (zero sidelobes, except for two small peaks at the edges), which implies nearly perfect $\sin^2(\pi f t_c) / (\pi f t_c)^2$ power spectrum. The length N of the code determines the phase of the elements. The amplitude sequence is determined by the sidelobe peaks and by the zero pattern of the z transform of the Huffman sequence. For a given sidelobe peak level there are 2^{N-1} different combinations. The zero pattern combination does not affect the autocorrelation (hence zero-Doppler cut of the ambiguity function), but does affect the ambiguity function at Doppler shifts other than zero and also the real envelope of the signal.

The same mainlobe width as an $M \times M$ MCPC signal will be obtained from an $N=M^2$ element Huffman code. An example of the envelope of a 25 element Huffman signal is given in Fig. 13. Clearly Huffman signals can be designed with much lower autocorrelation sidelobes than MCPC, but because of their perfect

$\sin^2(\pi f t_c) / (\pi f t_c)^2$ power spectrum shape, their spectrum use is less efficient. With regard to implementation, a Huffman signal has to be generated as one entity and then amplified using LPAs. On the other hand, a MCPC signal can be generated by passive power combination of M different signals, each one of constant amplitude.

Comparison with Costas Frequency Coding

Costas signals [6] achieve pulse compression by intrapulse frequency hopping. During any one of M code elements of duration t_b , only one of M frequencies is used, with no repetitions. The frequencies are separated by $1/t_b$. A Costas signal is the only other coded signal that achieves nearly rectangular spectrum, as does the MCPC signal, but Costas signals achieve that spectral efficiency while maintaining constant envelope. The first autocorrelation null of Costas signal is at t_b/M , like in MCPC. The autocorrelation sidelobe RMS level in Costas signals is generally slightly higher than in equally long MCPC.

Another way to compare between Costas signals and MCPC is to note that in order to transmit energy of $E = PMt_b$, a Costas signal requires a transmitter of power P , hopping over M frequencies, and using each frequency only for the duration of one t_b . On the other hand, a MCPC signal uses all the frequencies, all the time, by power combining M fixed-amplitude signals each with power P/M .

It is interesting to note that in the 5×5 MCPC signal described in Table 1, in the permutation with lowest sidelobes [3 5 2 1 4], isolating the 0° phase elements creates a Costas signal.

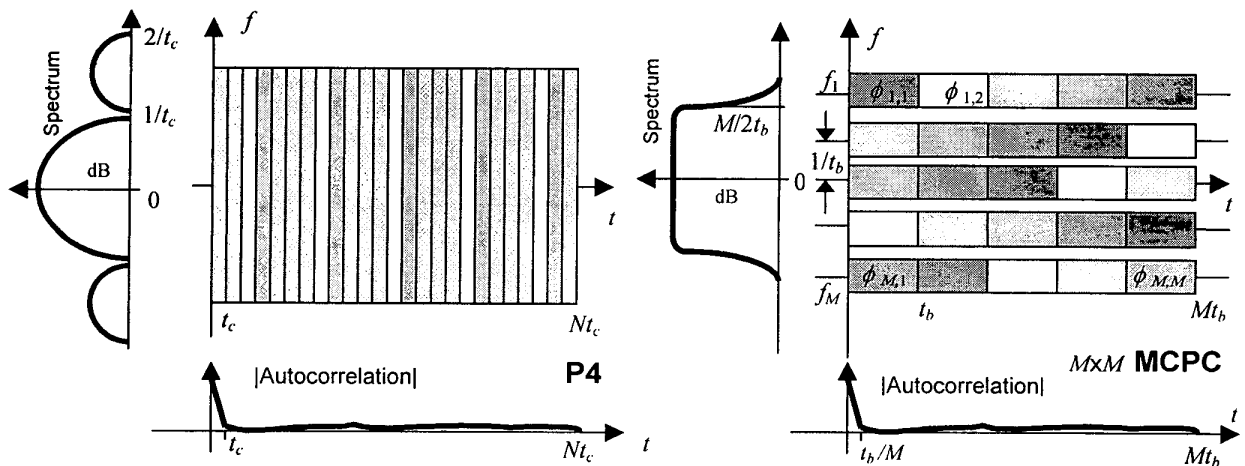


Figure 1. Schematic comparison between $M \times M$ MCPC and M^2 element P4

References

1. Le Floch, B. R. Halbert-Lassalle, and D. Castelain (1989), "Digital sound broadcasting to mobile receivers", *IEEE Trans. Consum. Elec.*, pp. 493-503.
2. Jankiraman, M., B.J. Wessels, and P. Van Genderen, "System design and verification of the PANDORA multifrequency radar", *Proc. of Int'l. Conf. On Radar Syst.*, Brest, France, 17 - 21 May 1999, Session 1.9.
3. Kretschmer, F.F. and B.L. Lewis (1983), "Doppler properties of polyphase coded pulse compression waveforms", *IEEE Trans. Aerosp. Electron. Syst.*, pp. 521-531.
4. Huffman, D.A. (1962), "The generation of impulse-equivalent pulse trains", *IRE Trans. Inf. Theo.*, pp. S10-S16.
5. Ackroyd, M.H. (1970), "The design of Huffman sequences", *IEEE Trans. Aerosp. Electron. Syst.*, pp. 790-796.
6. Costas, J.P. (1984), "A study of a class of detection waveforms having nearly ideal range-Doppler properties", *Proc. IEEE*, pp. 996-1009.
7. Popovic, B.M. (1990), "Complementary sets based on sequences with ideal periodic autocorrelation", *Electron. Lett.*, pp. 1428-1430.
8. Farnet, E.C. and G.H. Stevens (1990), "Pulse compression radar", *Radar Handbook*, 2nd edition, Skolnik, M., Ed., McGraw-Hill, New York, Ch. 10.
9. Golomb, S.W. (1992), "Two-valued sequences with perfect periodic autocorrelation", *IEEE Trans. Aerosp. Electron. Syst.*, pp. 383-386.
10. Tseng, C.C. and C.L. Liu (1972), "Complementary sets of sequences", *IEEE Trans. Inf. Theor.*, pp. 644-652.

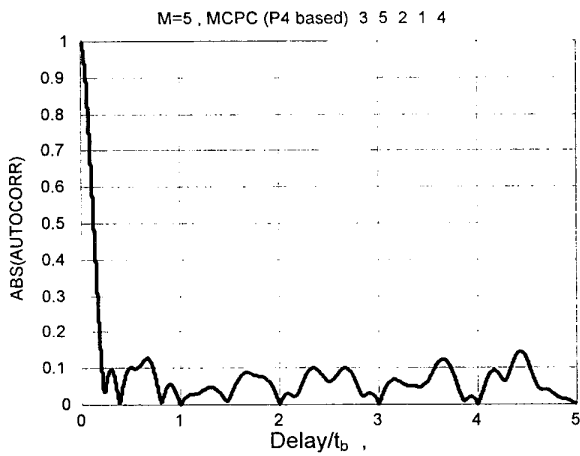


Figure 2. |Autocorrelation| of a 5x5 MCPC signal

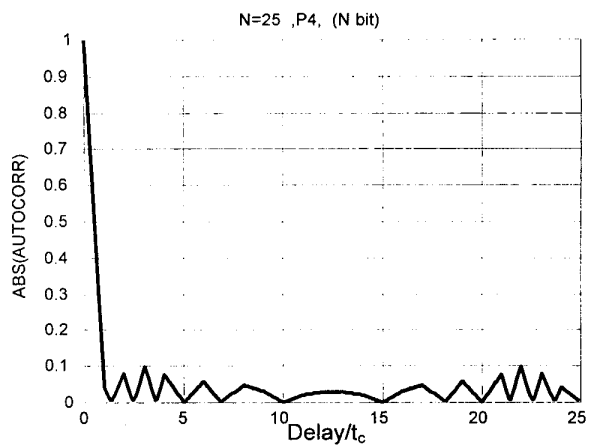


Figure 3. |Autocorrelation| of a P4 signal ($N=25$)

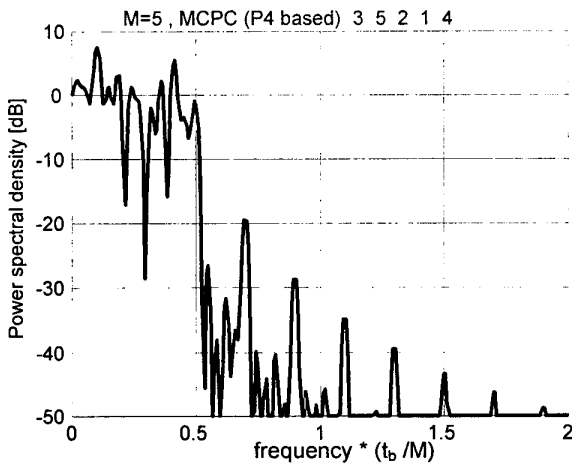


Figure 4. Spectrum of a 5x5 MCPC signal

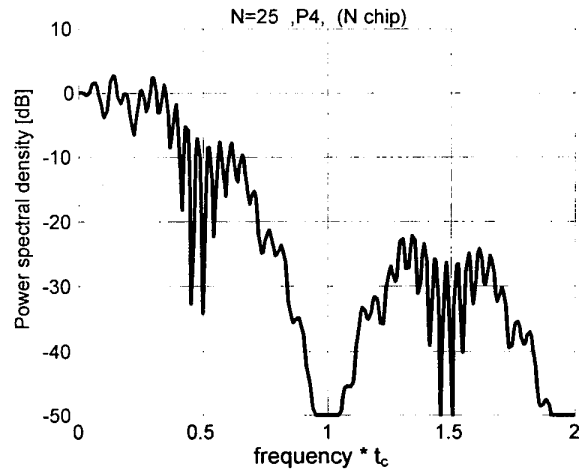


Figure 5. Spectrum of a P4 signal ($N=25$)

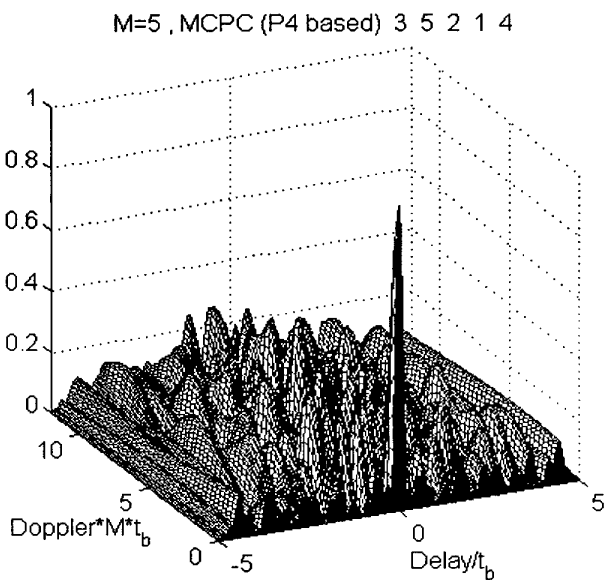


Figure 6. Ambiguity function of a 5x5 MCPC signal

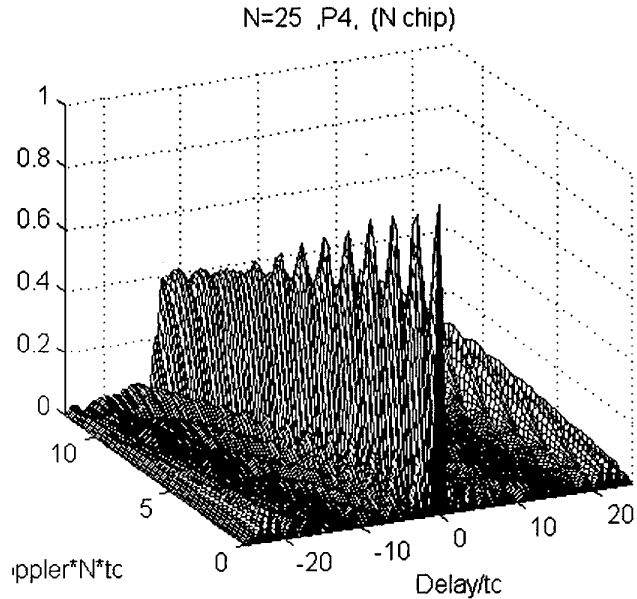


Figure 7. Ambiguity function of a P4 signal ($N=25$)

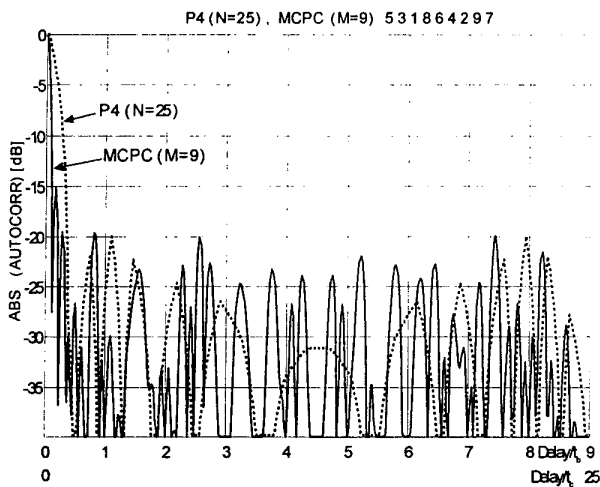


Figure 8. |Autocorrelation| of MCPC ($M=9$) and P4 ($N=25$)

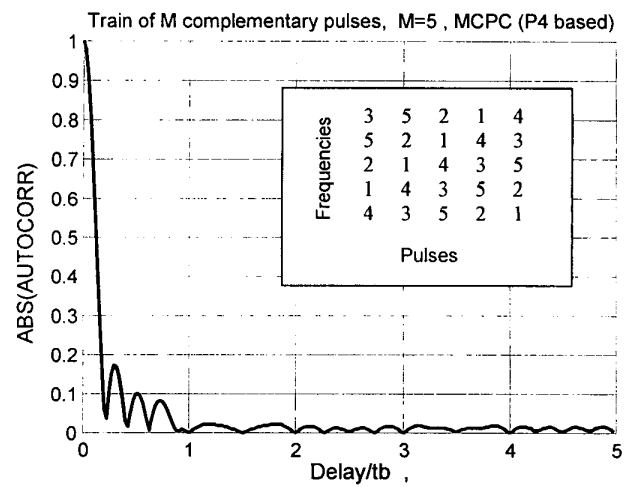


Figure 9. |Autocorrelation| of a train of 5 MCPC pulses

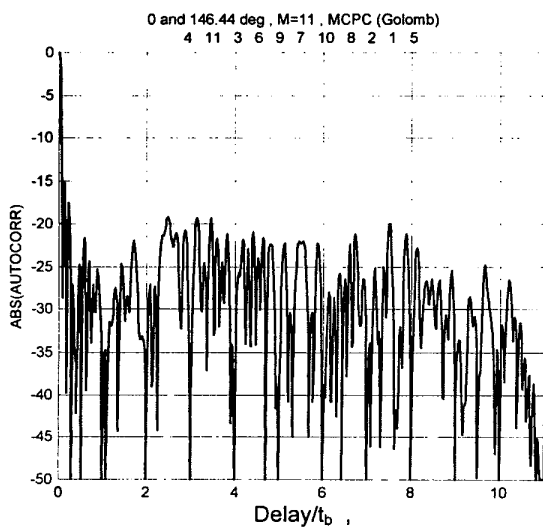


Figure 10. |Autocorrelation| of MCPC ($M=11$)

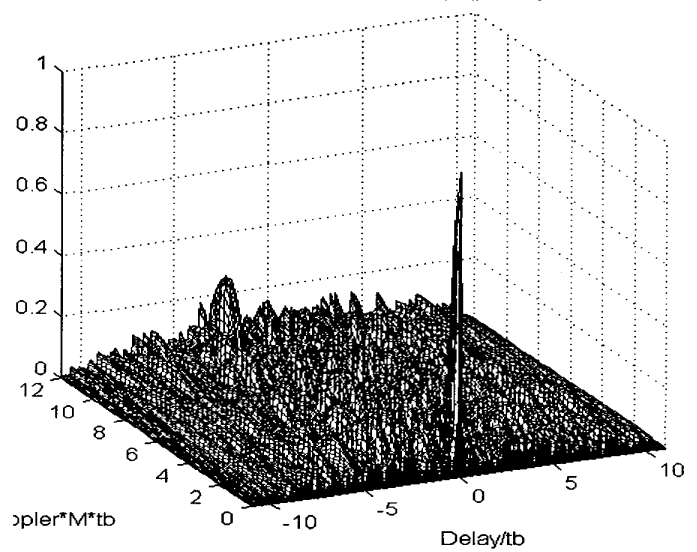


Figure 11. Ambiguity function of MCPC ($M=11$)

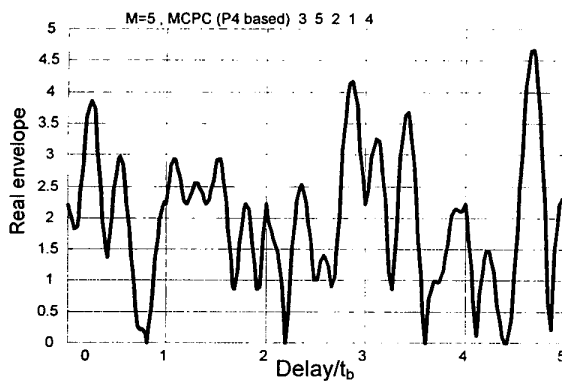


Figure 12. Real envelope of MCPC ($M=5$)

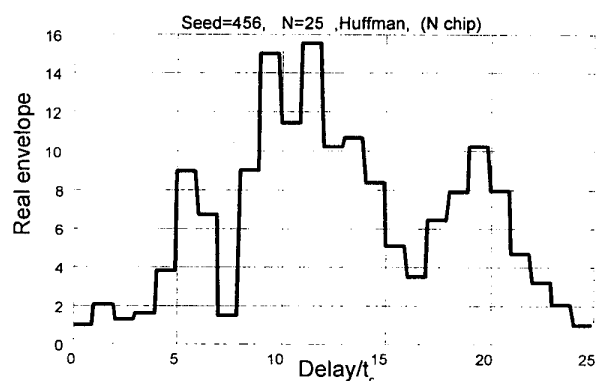


Figure 13. Real envelope of Huffman ($N=25$)